Optically monitored paramagnetic ion relaxation in an adiabatic demagnetization experiment*

C. A. Moore†
Department of Physics, University of California, Los Angeles, California 90024
(Received 18 February 1975)

Relaxation rates of the paramagnetic rare-earth ions Nd, Sm, and Er in ethylsulfate crystals have been measured as a function of magnetic field from 0–13 kOe at temperatures of 1.4 and 2°K using optical methods of detection. Nonequilibrium population differences were obtained by the rapid change of the magnetic field in a superconducting solenoid. Spin-memory measurements of the spin-lattice relaxation rate near zero field were possible for Nd and Sm ions. For crystals having a paramagnetic ion concentration greater than 3 at.% the relaxation behavior in the high-field region is affected by the phonon bottleneck. Theories appropriate to the prediction of the field dependence of spin-lattice relaxation rates, including the low-field and phonon-bottlenecked cases, are reviewed and used to interpret the data. Anomalous low-field rates, and some features of the optical methods of measurement are discussed.

I. INTRODUCTION

Optical methods to monitor the instantaneous populations of ground electronic states which are split by a magnetic field have been found useful to study the spin-lattice relaxation[1-5] and cross relaxation[6] of paramagnetic ions. The optical method, if combined with the use of pulsed microwaves to provide an initial population disturbance, suffers the restriction that the magnetic field is fixed by the microwave resonance condition, and the measured relaxation rate is characteristic of that magnetic field. An alternative to microwave pumping of the states is provided by a method which pulses the magnetic field. Populations which were established at thermal equilibrium at an initial value of the magnetic field are no longer in thermal equilibrium with the lattice for a short time after the magnetic field has been rapidly switched to a final value. If the switching of the magnetic field occurs in a time which is short compared to the spin-lattice relaxation time then the use of an optical method of detection to monitor the spin population allows a measurement of the spin-lattice relaxation rate. The demagnetization is adiabatic in the quantum-mechanical sense in which no transitions are induced by the changing magnetic field.[7] The measured relaxation rate is a characteristic of the final value of magnetic field because the relaxation is occurring between levels which are split by an energy determined by the final field. By varying the value of the final field the field dependence of the spin-lattice relaxation can be measured. Because of the requirement that the magnetic field must be pulsed in a time short compared to the spin-lattice relaxation time, conventional iron laboratory magnets cannot provide the switching field. For a number of years auxiliary field coils have been used.[1,2,8] The experimental results reported here were obtained by switching the current in a superconducting solenoid which can achieve high fields but has a sufficiently small inductance for it to be rapidly switched.

Two similar optical methods can be used to monitor the populations. The first is the rotation of the linear polarization of a light beam propagated through the sample in a direction parallel to the magnetic field[2,9] (Faraday rotation). The second is the absorption of circularly polarized light (circular dichroism) of a light beam propagated in a direction parallel to the magnetic field.[3,10] Both methods give rise to a signal which is largest in the region of a characteristic optical-absorption line of the ion, the former method reflecting the behavior of the dispersion, and the latter reflecting the absorption of the spectral line. The desired signal is a result of the population change which occurs during spin-lattice relaxation. Both methods give rise to similar signal strengths and suffer the same problems of signal to noise ratio inherent in the detection of a small signal change on a constant background of light striking the photomultiplier. Both methods have been used in this study.

The theoretical treatment of spin-lattice relaxation for rare-earth ions in crystals was accomplished by Orbach who predicted both the temperature[11] and the field dependence[12] of the relaxation of the ions. He postulated a model in which the modulated crystalline electric field of the lattice provided the mechanism for converting the Zeeman energy of the spins into thermal energy of the phonons. His predictions for the temperature dependence of the relaxation have undergone repeated verification, in particular, by the initial comprehensive experiments on rare-earth ions.[13-18] In those experiments it became obvious, in many cases, that the phonon bottleneck[13] sometimes caused deviations from predict-

ed behavior. Experimental verification of Orbach's prediction for the field dependence of the relaxation came more slowly than for the temperature dependence because the conventional microwave methods of detection did not readily adapt themselves to measurements at many different fields.[5,19-22] In addition, when the externally applied field is small, i.e., of the order of the local fields due to other paramagnetic ions (dipolar field) and of the nucleus (hyperfine field), the theoretical treatment becomes very complicated. However, this low-field case has been treated theoretically by Orbach for the Raman process[12] and by Huber for the direct process.[23]

This paper will review different theories appropriate to the prediction of the field dependence of the spin-lattice relaxation rate of Zeeman levels (spins) in experimental situations which include both low-field ($H<H_{\text{local}}$) and high-field cases. Theories of the phonon bottleneck will be treated to determine their predictions for the field dependence of phonon bottlenecked relaxation rates. Spin-spin interactions which may account for anomalously rapid low-field rates are discussed along with and a spin-memory technique which permits the measurement of the true low-field spin-lattice rates. The measurements of the relaxation rates of samarium (Sm), neodymium (Nd), and erbium (Er) ions in the lanthanum ethylsulfate (LaES) crystal will be interpreted in terms of the predictions of the foregoing theories, when they are applicable.

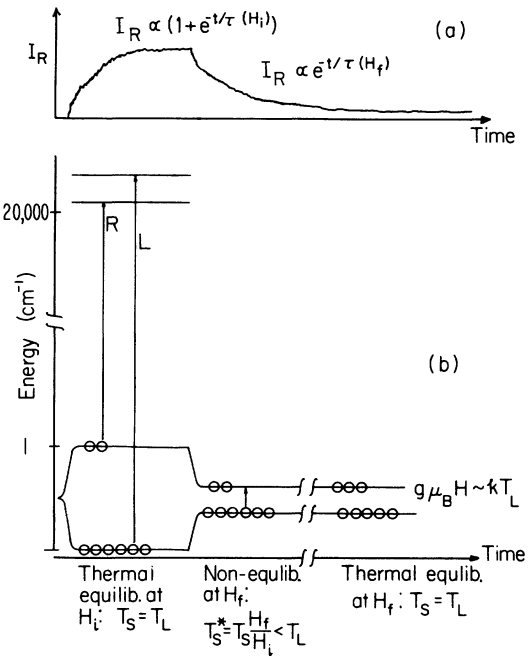

FIG. 1. Illustration of (a) signal observed and (b) energy levels, monitoring optical transitions and ground-state populations in the course of an adiabatic demagnetization experiment. T_S and T_L are the spin and lattice temperatures at thermal equilibrium and T_S^* the spin temperature immediately after demagnetization. R and L indicate right and left circularly polarized light. I_R is the intensity of right circularly polarized light transmitted by the sample.

II. EXPERIMENTAL METHODS

The population of a Zeeman level of the ground state of a paramagnetic ion in a crystal can be continuously monitored in the circular dichroism method by observing the intensity of circularly polarized light which is transmitted at a wavelength corresponding to an optical transition of the ion. The light is passed through a sample which is placed in the center of a superconducting solenoid immersed in a bath of liquid helium. As the magnetic field is pulsed the population of the electronic state changes, and this change is reflected in the intensity of light transmitted by the sample. Figure 1 illustrates pictorially the nature of the observed signal which results from the population changes of the electronic states of the ions in the sample. The energy-level diagram depicts the electronic states, their splitting, and their populations as a function of time during one cycle of the magnet. The circular dichroism method is based on the existence of selection rules which are valid for optical transitions of ions in crystals. These can be determined by group-theoretical methods[10] or by a direct calculation of the matrix element for the transition.[3] For the uniaxial ethylsulfate crystals the selection rules stipulate that circularly polarized light having a particular sense of rotation (right or left) monitors exclusively only one of the Zeeman states if the light is propagated parallel to the magnetic field and the c axis of the crystal. This selection-rule requirement, along with the fact that light which did not propagate along a principal axis would have its polarization altered, required these samples to be precisely oriented with the c axis along the bore of the magnet. Because optical transitions in the trivalent rare earths are only weakly allowed, the light can be used as a probe without significantly affecting the relative populations of the ground-state Zeeman levels. The weak optical transitions often require the samples to have a higher concentration of paramagnetic ion than is usually the case when electron paramagnetic resonance techniques are used. The samples were grown from rare-earth oxides with a purity of 99.99% or better. Signal-to-noise

ratio is optimized by use of a high-intensity light source and by the observation of an optical-absorption line which is sufficiently strong to absorb approximately 80% of the incident light.[6] The greatest signal occurs for large changes in the magnetic field, but since a large field change increases the phonon bottleneck the field change was restricted to that necessary to give a reasonable signal. Both H(initial) and H(final) were typically changed together to give a ΔH of approximately 2 kOe.

A block diagram of the experimental apparatus is illustrated in Fig. 2. The equipment was designed and constructed for prior spin-lattice measurements on the neodymium ion in lanthanum ethylsulfate (Nd:LaEs), and is more fully described elsewhere.[24] The solenoid consists of supercon T48-B wire wound on a 3-in.-long form with a $\frac{3}{8}$-in. bore. Light is passed along the bore and through the sample which is centrally placed. Current switching was accomplished by transistor circuits. When the transistor switch was turned off the magnet energy was discharged into a variable-load resistor wired in parallel with the magnet coil. The magnet inductance was 250 mH and the discharge time constant was usually 4 msec. The charging time constant was limited by current control requirements to a value of 125 msec. To avoid bubbling problems in the light path the liquid helium was pumped, hence data was restricted to temperatures below the λ point. The Dewar had windows which excluded liquid nitrogen from the light path. The apparatus in Fig. 2 was easily converted for a Faraday-rotation method of measurement by inserting a polarizer in front of the sample and an analyzer behind the sample. Magnet calibration was accomplished by measuring the Zeeman splitting of a dilute sample of Nd:LaES and comparing

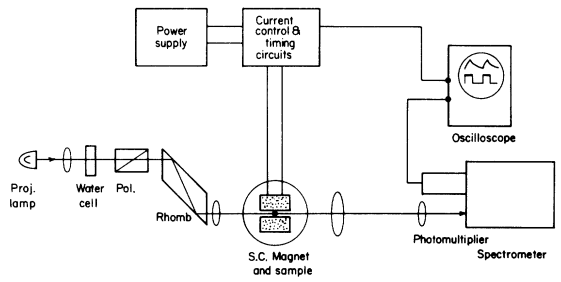

FIG. 2. Schematic diagram of apparatus used for optically monitoring the relaxation of paramagnetic ions in an adiabatic demagnetization experiment. The magnet inductance was 250 mH and the circuitry permitted operation at fields up to 13 kOe. The discharge time constant at high fields was limited to values greater than 4 msec. Charging time constant was 125 msec.

to known g values.[25] Calibration gave 1.12 kOe/A. The residual field of the magnet at zero current was measured with a cryogenic Hall probe. Although it gave rise to a significant field externally, (from which its existence was initially recognized) this residual flux-trapped field was found to be only 40 Oe at the center of the coil.

III. THEORY

A. Field dependence of spin-lattice relaxation

Orbach's treatment of spin-lattice relaxation provides a means for calculating from spectroscopically determined wave functions the relaxation rates of rare-earth ions in crystals in terms of some coefficients for the dynamic crystal field.[11,13,14] It predicts, for fields $H > H_{\text{local}}$ the field and temperature dependence of the relaxation rate for three processes: the direct, the Raman, and the Orbach processes. Orbach's theory can be summarized by the following formula for the field and temperature dependence of the relaxation (for the case of Kramers ions and where $g\mu_B H < kT$):

$$1/\tau = A(H)H^4T + B(H)T^9 + Ce^{-\Delta E/kT}, \qquad (1)$$

where the three terms represent the direct, the Raman, and the Orbach processes, respectively. In this formula ΔE represents the energy difference between the relaxing doublet and the nearest excited state participating in the Orbach process. The coefficients $A(H)$ and $B(H)$ summarize the strength of the interaction between the ion and the dynamic crystalline field. They are written as functions of the magnetic field because they depart from constants for values of H of the order of or smaller than the local fields.

At low temperatures the direct process, the direct emission (or absorption) of a phonon, is usually dominant. In this study T was always less than 2.2 °K, and the Raman and the Orbach processes were negligible for the ions investigated, except in the case of Sm for which the direct process (which varies as H^4 for $g\mu_B H \ll kT$) was dominated by the Raman process at low fields.

The validity of the Orbach theory has been tested by numerous microwave experiments which have served to determine empirically the constants A, B and C in the formula for the relaxation rate. This is generally achieved by curve fitting the temperature dependence of the data.[13-18] These experiments usually revealed good agreement with calculated estimates of the coefficients. The experimentally determined constants can be expected to predict the rates which one would mea-

sure in experiments at other applied fields so long as H exceeds the local fields.

To interpret experiments made at low magnetic fields, having strength of the order of the local dipolar and hyperfine fields, the more complicated theoretical treatment of the coefficients $A(H)$ and $B(H)$ must be used. The form of $B(H)$ for the Raman process was initially treated by Orbach[12] and the form of $A(H)$ for the direct process was calculated by Huber.[23] These calculations are difficult to evaluate for specific cases. Figures 3 and 4 represent an attempt to graphically depict the magnetic field dependence of the predicted relaxation rate which one might expect, on the basis of theory, to measure for a Kramers ion. In both figures, K is used to indicate the strength of the local field.

Orbach derives the following expression for the Raman-process relaxation rate at low fields[12]:

$$\frac{1}{\tau} = B_\infty T^9 \frac{H^2 + \mu H_{\text{hyp}}^2 + \frac{1}{2}\mu' H_{\text{dip}}^2}{H^2 + H_{\text{hyp}}^2 + \frac{1}{2}H_{\text{dip}}^2}. \qquad (2)$$

Figure 3 shows the rates expected from theory at a single low temperature in a hypothetical case for which the Raman process (having a high-field rate given by the baseline of the figure) is assumed to become competitive with the direct process at low fields. In this figure the direct process, depicted by the sharply rising rate at high fields, is included in the plot of low-field dependence of the Raman rate to introduce the note of reality that for low temperatures the direct process usually becomes dominant at higher fields. The Raman rate at low fields is plotted for various values of the parameter μ' of the Orbach paper. In Fig. 3, K represents the dipolar field only. Although the theoretical treatment includes the effects of both the dipolar and the hyperfine field, the full theory is not graphed because more parameters are included. If one were to plot the effect of the hyperfine field alone on the Raman relaxation rate, a similar plot to that of Fig. 3 would also result. Thus Fig. 3 depicts pictorially the effects on the Raman rate predicted by theories which include local fields.

Figure 4 illustrates the field dependence of the relaxation rate which is predicted by Hubers theory for the direct process. Unlike Fig. 3, it is assumed here that the Raman rate is negligible. In this plot, Huber's equation (35) is plotted where

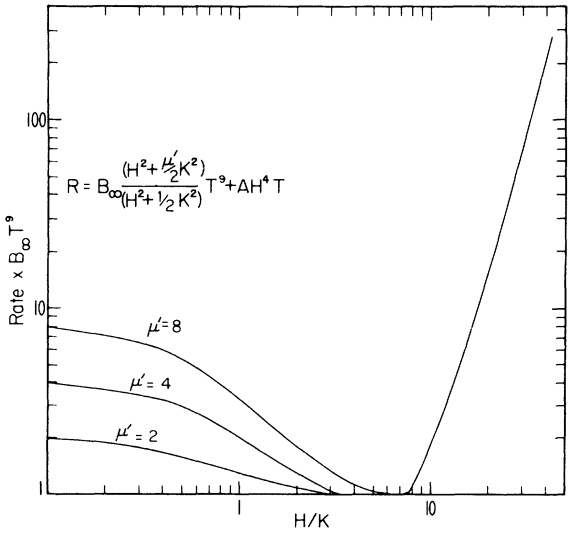

FIG. 3. Log_{10}-$\log_{10}$ plot of Orbach's dipole-field corrections to the Raman-process relaxation rate for various values of the parameter μ' (Ref. 12). Included in the plot is a direct-process rate to illustrate its eventual dominance at low temperature for high fields.

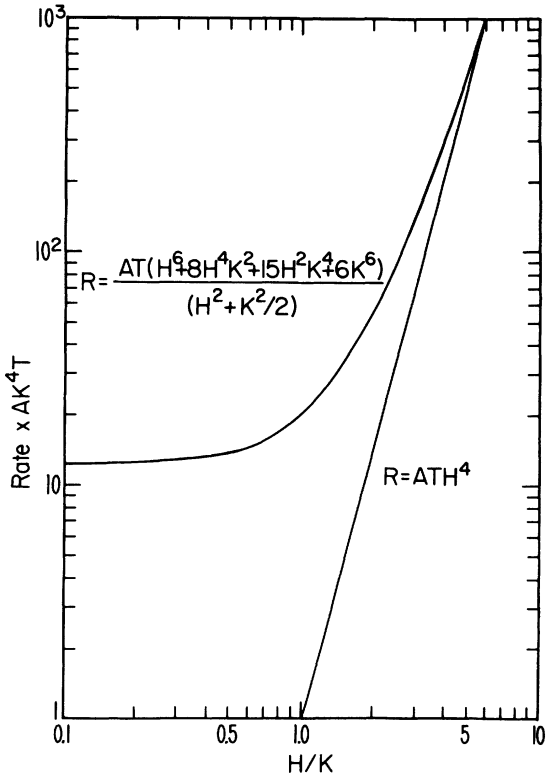

FIG. 4. Log_{10} -$\log_{10}$ plot of Huber's effective field correction to the direct-process relaxation rate for a Kramers ion (Ref. 23). K is the strength of the local dipolar field. Relaxation rate is plotted vs the ratio of applied to local field. For comparison, the plot includes the straight-line prediction of spin-lattice theory which does not include local-field corrections. The Raman rate is assumed to be negligible in this plot.

his two dipolar fields are assumed to be equal, and where parallel orientation of the field and crystal axis are assumed.[23] According to the assumptions of the Huber analysis $g_\perp$ is assumed equal to zero. Figure 4 is intended merely to depict graphically the general features which are theoretically expected when local-field effects are taken into account. The plots of Figs. 3 and 4 will be found useful for the interpretation of experimental results reported here.

B. Field dependence of phonon bottleneck

The interpretation of data in numerous spin-lattice relaxation experiments has revealed the presence of the phonon bottleneck.[6,9,13,26,27] It is a phenomenon which first arose in microwave heating experiments when a large number of spins relaxed by the direct process. A large number of phonons having an energy equal to the Zeeman energy of the spins are produced. Since these phonons are coupled to the spins, the observed spin-lattice relaxation rate is altered from that which would be observed in a weakly disturbed system by factors which include the relative number of spins and phonons, and the phonon lifetime τ_p. The appropriate coupled spin-phonon rate equations have been considered by a number of authors.[6,13,27-29]

In an adiabatic-demagnetization experiment the phonon bottleneck can also occur as it does in a microwave heating experiment. However, in the demagnetization experiment the spin temperature is initially reduced rather than increased as in the case of the microwave heating experiment. Instead of an increase there is a depletion in the number of phonons having an energy equal to that of the Zeeman energy of the spin in the final magnetic field. In the demagnetization case, however, the number of phonons at the Zeeman energy cannot be reduced without limit. Nevertheless, the same coupled spin-phonon rate equations again can be used.

Scott and Jeffries write the coupled equations[13] for the spin population difference n and the average phonon occupation number $\bar{p}$:

$$\dot{n} = \frac{-(n-n_0)}{\tau} - \frac{n}{\tau(\bar{p}_0+\frac{1}{2})}(\bar{p}-\bar{p}_0), \tag{3}$$

$$\dot{\bar{p}} = \frac{\sigma(\bar{p}_0+\frac{1}{2})}{\tau_p n_0}(n-n_0) - \frac{[\sigma(n/n_0)+1]}{\tau_p}(\bar{p}-\bar{p}_0), \tag{4}$$

where the zero subscript indicates thermal-equilibrium values, and where τ and τ_p are the unbottlenecked spin-relaxation time and phonon lifetime, respectively. The parameter σ is, for a given temperature and magnetic field, a constant called the bottleneck factor which can be written

$$\sigma = \frac{E_z/\tau}{E_p/\tau_p}, \tag{5}$$

where E_z and E_p are thermal-equilibrium Zeeman and (in band) phonon energies,

$$E_z = \tfrac{1}{2}\delta N_s \frac{1-e^{-\delta/kT}}{1+e^{-\delta/kT}}, \tag{6}$$

$$E_p = \rho_\delta(\Delta\delta)(\bar{p}_0+\tfrac{1}{2})\delta = \rho_\delta(\Delta\delta)\frac{1}{2}\frac{1+e^{-\delta/kT}}{1-e^{-\delta/kT}}\delta. \tag{7}$$

Here δ is the Zeeman energy of the ion, ρ_δ is the density of phonon states, $\Delta\delta$ is the bandwidth of the spins (and hence phonons), and N_s is the number density of spins in the sample.

In general, the solution of the nonlinear coupled equations is characterized by an initial decay rate τ^{-1} and a final decay rate given by the equation[28]

$$r = [\tau(\sigma+1)]^{-1}. \tag{8}$$

It is the latter rate which characterizes the tail of the relaxation and is most readily observed.

In the case of a severe bottleneck[13] ($\sigma \gg 1$),

$$r \approx \frac{1}{\tau\sigma} = \frac{E_p}{E_z}\frac{1}{\tau_p}, \tag{9}$$

and Eqs. (6) and (7) can be used to find both the temperature and field dependence of the bottlenecked rate. In the limit $\delta \ll kT$,

$$r \approx 1/\tau\sigma = 6k^2(\Delta\delta)T^2/N_s\pi^2 v^3\hbar^3\tau_p \equiv DT^2 \tag{10}$$

shows the characteristic T^2 dependence of the phonon strongly bottlenecked rate.[13] For our purposes it should be noted that this rate is explicitly independent of magnetic field; however, there may be further field and temperature dependence contained in the phonon lifetime τ_p which is a parameter appearing in the expression for D. A number of interesting processes might determine the phonon lifetime. These processes can be grouped into two categories: those which redistribute phonon energy into the whole spectrum of phonons, and those which involve the transmission of phonons across the crystal–liquid-helium interface. Some of the former are reviewed by Stoneham[29] and by Faughnan and Strandberg,[28] while the latter are discussed in review articles on the phenomenon of Kapitza resistance.[30-32] In some cases Kapitza resistance expressions describing the decay of the heat energy of the whole spectrum of acoustic phonons have been used to interpret the temperature dependence of some strongly bottlenecked spin-lattice relaxation data.[26] The processes which determine

the phonon lifetime have temperature and phonon-energy dependences which might profitably be studied by a phonon-bottlenecked relaxation experiment which can excite a narrow band of phonons at variable energies. The processes reviewed in Refs. 28 and 29 reveal differing energy and temperature dependences for phonon-decay mechanisms such as anharmonic scattering, diffusion to lattice defects, and impurity scattering which can be used to interpret the experimental results. Consideration of the Khalatnikov theory of Kapitza resistance,[30] when applied to the excitation of a narrow band of phonons, gives a temperature- and field-independent phonon lifetime which does not predict the observed dependence. However, recent studies have made considerable advances over the Khalatnikov theory in the understanding of Kapitza resistance, revealing the importance of phonon dissipation due to surface effects which may result in still other predictions for the field and temperature dependences of the phonon lifetime.[31,32]

The use of Eq. (10) is only appropriate for the strongly bottlenecked ($\sigma \gg 1$), high-temperature case. For other cases, Eq. (8), which is valid for all values of σ, should be used. We are specifically interested in those bottleneck parameters of order one for which the relaxation rates are not drastically reduced from the unbottlenecked rate, the situation most commonly encountered in this study. We therefore investigate the field dependence predicted by Eq. (8), and find that it shows a complex field dependence quite independent of any contributions from the field dependence of the phonon lifetime. Equation (8) describes a rate which can be expressed

$$r = [\tau(\sigma + 1)]^{-1} = r_u r_b/(r_u + r_b), \tag{11}$$

where r_b and r_u are defined by the strongly bottlenecked and unbottlenecked rates which (for Kramers ions) have field and temperature dependences given by[13]

$$r_b \equiv 1/\tau\sigma = D'\delta^2 \coth^2\delta/2kT \tag{12}$$

and

$$r_u \equiv 1/\tau = A'\delta^5 \coth\delta/2kT, \tag{13}$$

where

$$D' = 3(\Delta\delta)/2N_s \pi^2 v^3 h^3 \tau_p. \tag{14}$$

Expressions (12) and (13) exhibit the familiar rates, $r_b \simeq DT^2$ and $r_u \simeq AH^4T$, respectively, in the high-temperature limit. In an experiment in which the field is varied, the relative magnitude of the rates r_b and r_u varies, giving the behavior for Eq. (11) shown in Fig. 5 which is a graph of the rate r vs $\delta/2kT$ on a $\log_{10}$-$\log_{10}$ plot. For a given temperature $\delta/2kT$ is directly proportional to magnetic field, so except for that proportionality the plot of Fig. 5 is the same as those used to exhibit the data of these experiments. In Fig 5, an unbottlenecked rate r_u is represented by the steeply rising straight line. At low fields this rate is too slow to give rise to phonon heating, but as the field increases the direct process rate becomes comparable to the extreme phonon-bottlenecked rate $(\tau\sigma)^{-1}$, which has the nonzero constant value DT^2 in the high-temperature approxi-

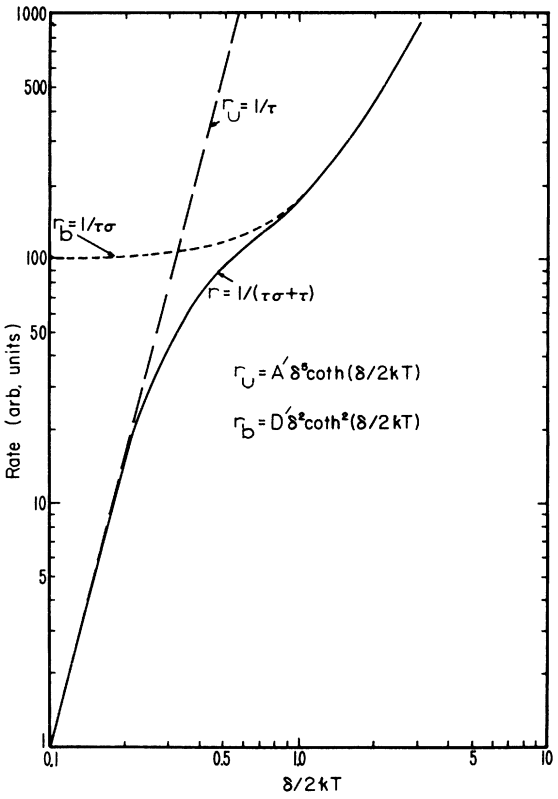

FIG. 5. Log_{10}-$\log_{10}$ plot of the field dependence of the predicted relaxation rate in the region where phonon heating effects become apparent. A single temperature is assumed. Field strengths are related to the abscissa by use of the relation $g\mu_B H = \delta$. The plot includes both the "high-temperature" ($\delta < 2kT$) and "low-temperature" ($\delta > 2kT$) limit. The coefficients A' and D' will vary from sample to sample. The solid curve indicates the predicted rate $1/\tau(\sigma+1)$. The dashed curve indicates the characteristic form of an unbottlenecked spin-lattice rate. The dotted curve indicates the form of the severe bottleneck rate $1/\tau\sigma$ which only dominates the relaxation when very much slower than the spin-lattice relaxation rate $1/\tau$. For a temperature of 1.4 °K the transition to low-temperature behavior, $\delta = 2kT$, occurs when $\delta = 2$ cm^{-1}, a condition approached in this study only in the case of the neodymium ion.

mation (low fields). The measured rate r then departs from the unbottlenecked rate because of phonon heating. Fields for which $r_u \gg r_b$ reveal the limiting behavior that the measured rate r is that of the extreme phonon bottleneck rate $r_b = (\tau\sigma)^{-1}$. At fields for which $\delta > 2kT$, this rate r_b no longer has the field-independent value DT^2 because the high-temperature assumption is violated.

In summary, the solid curve of Fig. 5 exhibits the general features of the field dependence of the relaxation rate having the form $[\tau(\sigma+1)]^{-1}$. It shows a slope which can be less than the H^4 dependence (for Kramers' ions) predicted from spin-lattice theory. The exact form of this curve will vary between samples depending on the relative magnitude of the rates r_b and r_u. Departures from this curve can reveal information on the field and temperature dependence of the phonon lifetime in Eq. (14).

C. Spin-spin interactions

Table I contains estimates of averaged dipolar and hyperfine fields evaluated for the ions studied in this work. These estimates, based on a formula from Van Vleck,[33] the lattice sum of Daniels,[34] and spin-Hamiltonian parameters from the literature,[25] indicate the strength of the local fields H_L. When, in the demagnetization experiments reported here, the final field was set to values $H_f \sim H_L$, the optical signal was observed to decay at rates consistently more rapid than those predicted from local-field theories of spin-lattice relaxation,[12,23] increasing abruptly as the setting of final field was reduced. These anomalous rates are believed to represent the results of spin-spin interactions rather than spin-lattice relaxation.

In an analysis of the exchange of energy between Zeeman and dipole energy reservoirs, Kronig and Bouwkamp[35] proposed the following field dependence for the spin-spin relaxation rate:

$$w = (1/T_2)e^{-H^2/H_L^2}, \tag{15}$$

where T_2 is the spin-spin relaxation time at energy overlap. Bloembergen *et al.*, formulated a theory for the exchange of energy between spin systems having nonoverlapping energy levels in their classic paper on cross relaxation.[36] Their expression for the cross-relaxation rate between two spins species labeled by α and β is

$$w = (1/\hbar^2) H_{\alpha\beta}^2 g_{\alpha\beta}, \tag{16}$$

where $H_{\alpha\beta}$ is the matrix element of the interaction and $g_{\alpha\beta}$ is the overlap function of the respective frequency distributions. For Gaussian distributions centered at $\nu_\alpha = 0$ and $\nu_\beta = g\mu_\beta H/h$, this expression gives a rate having the dependence given by Eq. (15). However, the factor $g_{\alpha\beta}$ depends on wings of the frequency distributions which may not be Gaussian. Equation (16) would be appropriate to determine the rate at which energy is transferred between electronic and nuclear spins for final fields approaching the value H^* at which energy conserving transitions can occur between equally spaced hyperfine levels. Population changes induced by such spin-spin interactions have been experimentally investigated. In their paper, Abragam and Proctor[7] discuss spin-memory experiments which used electron-spin resonance at a high field to detect population changes among hyperfine levels which had been induced by energy-conserving spin-spin interactions when the applied field was temporarily set to the field H^* much smaller than the resonance field. Those experiments differed fundamentally from the ones reported here because individual hyperfine transitions were observed, whereas the optical method of this study detects the totality of the populations of the hyperfine levels associated with either the $M_s = -\frac{1}{2}$ or $M_s = +\frac{1}{2}$ Zeeman states. If, at the field H^*, the hyperfine states compose a ladder of equally spaced levels, the establishment of a Maxwell-Boltzmann population distribution in these states would alter the population of individual hyperfine levels from their high-field thermal-equilibrium values. However, it would leave the total population of the states derived from either the (high-field) $M_s = -\frac{1}{2}$ or $M = +\frac{1}{2}$ states unchanged from its high-field value.[7]

TABLE I. Estimates of local fields (in Oersteds) of some rare-earth ethylsulfates.

	$K_{dd} = \left(\frac{\mu_B^2(g_\parallel^2 + g_\perp^2)s(s+1)}{\Sigma K_{ij}^6}\right)^{1/2}$	$K_{hf} = \frac{I}{g_\parallel \mu_B}[\frac{1}{2}(A^2+B^2)]^{1/2}$
Sm^{147}	39	2310
Sm^{149}	39	1880
Nd^{143}	187	643
Nd^{145}	187	402
Er^{167}	408	1148

Hence no net change in the optical absorption would be expected for equally spaced levels from population changes alone. If, however, the ground states at the field H^* are caused to be admixtures of the $M_s = \pm\frac{1}{2}$ states a failure of the optical selection rules is expected. This change in selection rules can also be interpreted as a result of the effective field no longer being oriented along the crystalline axis. This would cause a change in the optical absorption to be observed upon demagnetization to final fields $H_f \sim H^*$. Such optical signals cannot be interpreted to indicate spin-lattice rates, but may indicate the field dependence and rate of the spin-spin interactions.

The relatively slow spin-lattice relaxation rates of nuclear spins have permitted the measurement of spin-spin effects in spin-memory experiments[7,37] in which the amount of magnetization is measured before and after the field is dropped to a value $H \sim H_{\text{dip}}$. The complexity of the dipolar interactions permitted in this many-body problem requires an analysis in terms of the spin-temperature concept.[37] The spin-memory experiments of Abragam and Proctor showed that nuclear spins, originally polarized at high field, retained that polarization after the applied magnetic field had been reversibly cycled in times less than the spin-lattice relaxation time through a low field where spin-spin interactions between identical spins were allowed to take place. The spin-temperature analysis of Abragam and Proctor led them to conclude that energy of identical spins can be reversibly transferred between the Zeeman and dipolar reservoirs in a spin-memory experiment which is conducted in a time short compared to the spin-lattice relaxation time. This result is the basis for the spin-memory experiments conducted here in which the magnet current is briefly dropped to zero. For electronic spins the spin-lattice rates are such that information on spin-lattice relaxation at low fields can be obtained by spin-memory experiments in which the magnetic field is cycled on time scales of approximately one second. In this case the spin populations are measured after a return to a high field where the optical selection rules are known to be valid. Unlike the rates measured in the low-field region by the demagnetization method, the spin-memory rates are here regarded as truly representing spin-lattice relaxation rates.

IV. EXPERIMENTAL RESULTS AND DISCUSSION

Relaxation measurements were made on a number of different rare-earth ions in the ethylsulfate crystal. Both Faraday-rotation and circular-dichroism techniques of detection were used. The spin-lattice rates obtained from both optical methods were in agreement for each sample. In all cases, the relaxation rate was measured only for the magnetic field parallel to the principal axis of the crystals because of the requirements of the optical technique.

The circular-dichroism method of detection was generally preferred to the Faraday-rotation method because line shifts during the collapse of the magnetic field gave misleading signal strengths and polarity reversals in the latter method. These are illustrated by Figs. 6 and 7. Figure 6 shows the spectral dependence of the Faraday-rotation signal from an erbium sample, and Fig. 7 presents the explanation of the signal envelope of Fig. 6 in terms of the dispersion functions[38] associated with the two Zeeman-split states. Figure 7(c) shows the spectral dependence of the Faraday-rotation signal which is proportional to the difference in the index of refraction $n_- - n_+$ of the two Zeeman states. As a function of time the Faraday signal at any optical frequency ω proceeds rapidly (while the field collapses) from the solid to the dashed curve of Fig. 7(c), and then, at the spin-lattice decay rate, from the dashed curve to the baseline. These two stages are related to line-shift and population-change effects, respectively.[39] Figure 6 shows a similar asymmetric signal profile to that predicted by Fig. 7(c) for each of two spectral lines of erbium, but superimposed on the normal spectral absorption curve. In relaxation measurements the Faraday signal showed the same temporal behavior and polarity changes as a function of wavelength which are predicted in Fig. 7(c). These wavelength-sensitive effects made the Faraday method

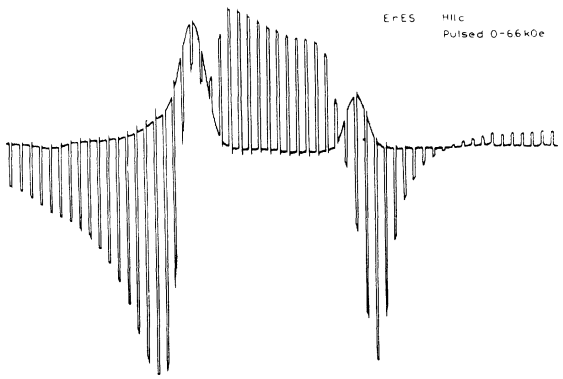

FIG. 6. Faraday-rotation signal superimposed on the absorption spectrum of ErEs in the vicinity of the 5415- and 5407-Å lines of Er. The spectrum was slowly scanned while the field was pulsed on and off. The Faraday signal reflects the behavior illustrated in Fig. 7 and consists of both line-shift and relaxation effects.

more difficult to use and interpret than the circular-dichroism method.

In the case of Sm and Nd ions, a novel spin-memory technique was applied to obtain the spin-lattice relaxation rate of electronic spins near zero field. Similar techniques have usually been restricted to the study of nuclear spins.[7,37] The relaxation rates of Sm and Nd were sufficiently slow at low fields that the solenoid current could be switched off and on again in a time shorter than the spin-lattice relaxation time permitting a signal recovery technique to measure the degree of spin memory. By measuring the strength of the optical-absorption signal immediately after current turn on as a function delay time at zero current, one could ascertain the population loss during the delay, i.e., the relaxation rate at fields corresponding to zero current in the solenoid. Because the superconducting magnet had a trapped-flux field of approximately – 40 Oe when it was in a zero current condition, the spin-memory rates correspond to this applied magnetic field which is smaller than the local fields. The residual magnetic field was measured and profiled with a cryogenic Hall probe and had an orientation at the center of the bore in a direction opposite to the original field. External to the magnet, however, the dipolar residual field of the whole solenoid had an orientation parallel to the original field.

The method for obtaining spin-memory relaxation rates is illustrated in Fig. 8 which shows oscilloscope traces of the optical-recovery signal of SmES as the magnet was repeatedly switched between current on and current off conditions. From such spin-memory measurements the zero-current relaxation rates were determined by plotting the initial signal recovery versus delay time at zero current. Such measurements were

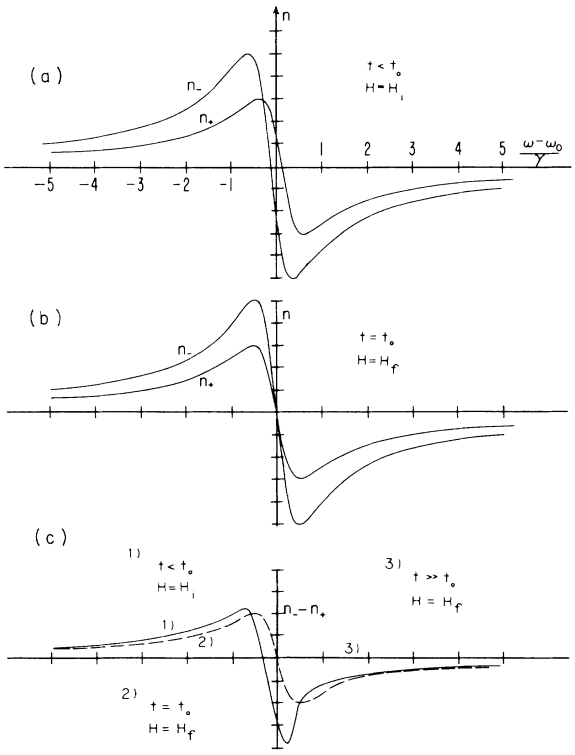

FIG. 7. Dispersion of the indices of refraction for left and right circularly polarized light in the vicinity of an optical absorption line arising from a transition between Zeeman doublets. The difference in amplitude reflects the difference in population in the upper, +, and lower, −, Zeeman levels of the ground state at low temperatures. The indices are shown in (a) at a large magnetic field and in (b) immediately after a rapid demagnetization to zero field. The Faraday-rotation signal, proportional to the difference $n_- - n_+$, is shown in (c). The experimentally observed Faraday-rotation signals exhibited the spectral and temporal behavior illustrated here.

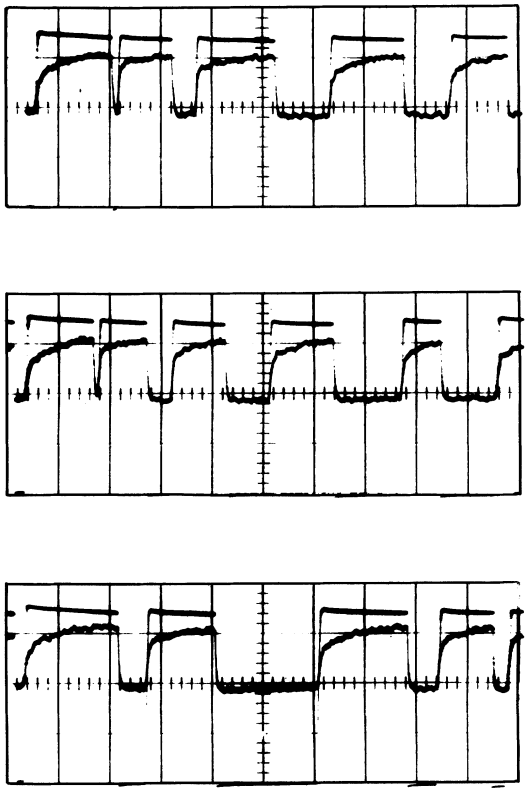

FIG. 8. Oscilloscope display of the magnet current and the optical circular dichroism signal in the spin-memory measurement of the relaxation of the Sm ion at zero current. From these traces a plot of the initial optical signal recovery vs delay at zero current revealed the relaxation time. Sweep speed is 2 sec/div.

restricted to operation between fields for which the spin-lattice relaxation times were longer than the current recovery time of 125 msec.

Figure 9 presents the experimental results for the field dependence of the relaxation rate of the Sm ion diluted in the LaES crystal. In the high-field region the agreement between experimental points from this study and those of Larson and Jeffries,[16] in addition to the H^4 dependence of the data, indicate that the relaxation of the Sm ions in this dilute sample is exhibiting the (high) field dependence predicted by spin-lattice relaxation theory, and that the phonon bottleneck is not affecting the measured rate. The high-field data for this ion thus show satisfying agreement with expected behavior, indicating that the experimental techniques are essentially correct. In the low-field region the data are not so simply understood in terms of established theories of spin-lattice relaxation. However, the relaxation measurements on the different ions of this study reveal a pattern which permits a consistent interpretation of the low-field measurements. For the Sm LaES sample the data in the low-field region ($H<2$ kOe in Fig. 9) obtained by the demagnetization method exhibits an increase in rate as the final field is reduced. A spin-memory measurement was attempted for this sample, but the relaxation rate at low fields was apparently too fast to give a measurable rate with this apparatus. This was an unexpected result because a measurable spin-memory rate was found for the same ion in the more concentrated crystal, SmES. The increased rates measured at low fields by the demagnetization method were found to be a characteristic of all the ions studied. As in the case of the other ions studied here, the upturn in the low-field rate for Sm occurred for applied field strengths of the order of the local hyperfine field of the ion (Table I). The increased rates are, thus, apparently related to the local fields, however the field dependence shown by the low-field rates are generally in disagreement with the theoretical predictions of the local-field theories of spin-lattice relaxation[12,23] (Figs. 3 and 4). Furthermore, the fast rates are in some cases contradicted by spin-memory rates measured in this study. Because of the contradictions with spin-lattice relaxation theory and with some spin-memory measurements, the generally occurring fast low-field rates are not believed to represent true spin-lattice interactions as discussed in Sec. III C. In this view the change in optical absorption for $H_f \approx H_L$ arises because the local fields produce an environment for different ions which departs from the C_{3h} crystal-field symmetry of the rare-earth ion in an external field parallel to the crystal axis. These local-field spin-spin interactions can lead to electronic states which no longer obey the selection rules for left and right circularly polarized light which is the basis for the optical method of detecting spin populations. The low-field relaxation rates which were observed for the samples studied here do not fit the exponential field dependence of Eq. (15) for the spin-spin relaxation rate. Equation (16) for the cross-relaxation rate might appropriately describe the field dependence of the observed spin-spin rates. However, the use of that equation is limited by an incomplete knowledge of the field dependence of the overlap function $g_{\alpha\beta}$ which is sensitive to the shape of the wings of the frequency distributions. The overlap is complicated by the hyperfine structure which is not resolved with the optical method.

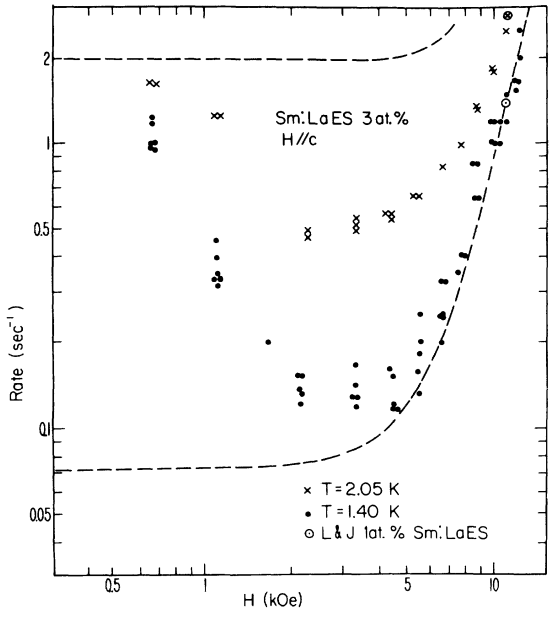

FIG. 9. Log_{10}-log_{10} plot of the experimental results for the field dependence of the relaxation rate of 3-at.% Sm:LaES. Good agreement is obtained with the encircled data points which show the data obtained by Larson and Jeffries in an x-band microwave experiment for the temperatures used here (Ref. 16). The dashed curves represent a graph of Eq. (1) using the constants which Larson and Jeffries obtained by fitting the temperature dependence of their data. It is seen that the Raman process, having a flat field dependence, is predicted to dominate the direct process for relaxation at low fields. For this concentration an H^4 high-field dependence was observed.

The observation of rapid spin-spin rates in the low-field region in the demagnetization experiments does not mean that the spin system has achieved thermal equilibrium with the lattice on

that time scale. As discussed in Sec. III C, consideration of the topic of spin temperature has shown that dipolar interaction between spins cannot directly contribute to the establishment of thermal equilibrium of spins with the lattice.[7,37] Those studies showed that energy of nuclear spins can be reversibly transferred between Zeeman and dipolar reservoirs during adiabatic demagnetization and remagnetization, a result of importance to the spin-memory method of measurement used in this study. These considerations substantiate the conclusion that the rapid rates found at low fields should not be interpreted as true spin-lattice rates, but may reflect spin-spin rates. However, the slower rates obtained by the spin-memory method in other samples to be discussed can be regarded as the true spin lattice rates.

An alternative hypothesis for the fast relaxation rates at low fields is that they might arise from cross relaxation[36] to fast-relaxing impurity ions, a process which might preferentially occur at low fields where the different paramagnetic ions, having field-independent linewidths and hyperfine splittings, would be likely to have overlapping energy levels. In this view the rapid rate ultimately represents spin-lattice relaxation but would not be expected to show the dependence predicted by theory for an isolated ion. However this explanation is not thought to account for these quite generally occurring observed rates. Consideration of the rate equations for such a process shows that, even when the cross-relaxation rate is fast, the effective spin-lattice relaxation rate may not be substantially altered because of its dependence on the relative concentration of ions,[6,36] which should be quite low in the samples used here. Moreover, in some cases the cross-relaxation explanation is considered unlikely because of the experimental observation of slow relaxation rates by the spin-memory method.

Figure 10 presents the results of measurements of the field dependence of the relaxation of the Sm ion in SmES. Comparison with Fig. 9 reveals that high-field data for the concentrated crystal depart from that for the dilute 3 at.% SmLaES sample, no longer exhibiting the H^4 dependence predicted by theory. The slope of the data indicates a rate varying approximately as H^2 out to the apparatus limit of 13 kOe. This departure of the data from predicted behavior is interpreted as a manifestation of the phonon bottleneck. Comparison with the data of Fig. 9 indicates that the bottleneck parameter is of order one, hence the use of Eq. (11) rather than Eq. (10) is appropriate. For the fields used here the high-temperature approximation is valid for the Sm ion, and the

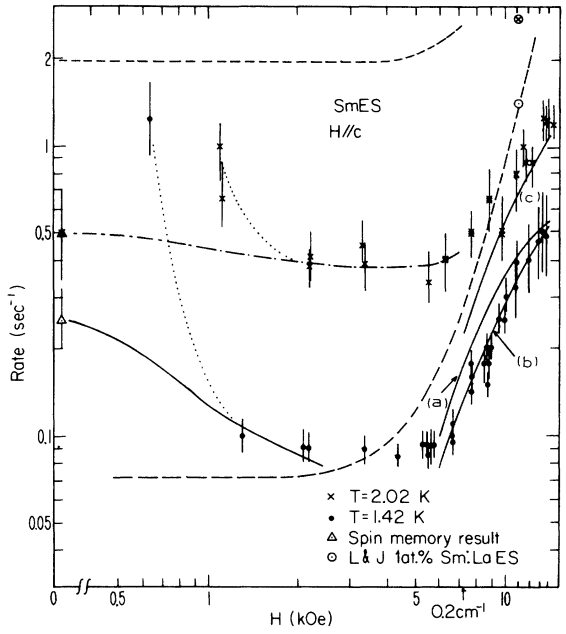

FIG. 10. Log_{10}-log_{10} plot of the experimental results for the field dependence of the relaxation rate of SmES. The encircled data points and dashed curve represent the results of Larson and Jeffries (Ref. 16). The results of spin-memory measurements of the relaxation rate near zero field are shown by triangular data points. The curves drawn in the high-field region are fits to the bottlenecked data based on Eq. (11) as explained in the text.

field-independent expression, Eq. (10), can be used for r_b appearing in Eq. (11). In Fig. 10 the solid curve (a) in the high-field region is an attempt to fit the data by Eq. (11) in which the unbottlenecked direct-process rate of Ref. 16 and a field-independent value of 0.6 sec^{-1} for r_b are used. To obtain this fit the Raman process of Ref. 16 was omitted, a decision justified by the rather poor agreement of the data with the low-field rates (indicated by the dashed curves of Figs. 9 and 10) which would be anticipated if a Raman process of that magnitude were included. The form shown by curve (a) is in disagreement with the curvature shown by the data, indicating that the assumption of a field-independent phonon lifetime may not be appropriate. Attempts were therefore made to fit the data by assuming phonon lifetimes which varied as powers of the magnetic field. Curve (b) shows the result when a inverse linear dependence of the phonon lifetime is assumed. This fit again represents the phonon bottlenecked rate given by Eq. (11), but the coefficient D appearing in the expression (10) for the rate r_b has been modified to explicitly intro-

duce a field dependence for the phonon lifetime. The curve (b) thus represents Eq. (11) with $r_b = 0.043\, H\,\mathrm{sec}^{-1}$, where H is in kOe. The resulting curve is seen to provide a better fit than that obtained using a field-independent phonon lifetime. Curve (c) was obtained by extrapolating the rates r_u and r_b by their respective T and T^2 dependences. The quality of the fit indicates that the phonon lifetime is approximately independent of T. These field and temperature dependences for the phonon lifetime are consistent with the mechanism of diffusion to lattice defects.[29] The mechanism of anharmonic scattering is ruled out by its predicted T^6 dependence for the rate r_b.[29]

In the low-field region of Fig. 10, the data obtained by the demagnetization method show an upturn in the measured rate (indicated by the dotted lines) similar to that encountered in the 3-at.% Sm data of Fig. 9. The onset of the upturned rate occurs at the same value of magnetic field, and agrees with the estimate of the hyperfine field of this ion (Table I). This is consistent with the viewpoint that this upturn in measured rate is due to spin-spin interactions between hyperfine levels. The distinctive feature the low-field data of Fig. 10 is the presence of the spin-memory measurements indicated by the triangular data points. These measurements, as discussed previously, are obtained by a different method from the demagnetization method used to obtain the rest of the data, and are not subject to the criticism that the optical signal is being measured at a field which is of the same magnitude as the local field. For this reason they are interpreted as a measure of the true spin-lattice relaxation rate. The solid curve drawn in the low-field region through the 1.4 °K spin-memory datum point shows an Orbach local-field correction to the Raman rate of Larson and Jeffries which has the paramaters $\mu = 3$ and a local field of 800 kOe, a value smaller than the estimate in Table I. However, the spin-memory data show a T^2 rather than the T^9 dependence expected for the Raman process, and, as stated earlier, the disagreement of the 2.02 °K data in the low-field region with the predicted Raman rate indicates that a Raman process of that magnitude may not occur.

Figure 11 presents the experimental results for the field dependence of the relaxation of 5-at.% Nd in LaES. The neodymium ions in this sample had natural isotopic abundancies, unlike the enriched ^{142}Nd sample to be discussed later. The results of microwave measurements of other studies,[6,13] plotted in the figure for comparison, do not show a spin-lattice rate having an H^4 dependence. However, the x-band data fall into

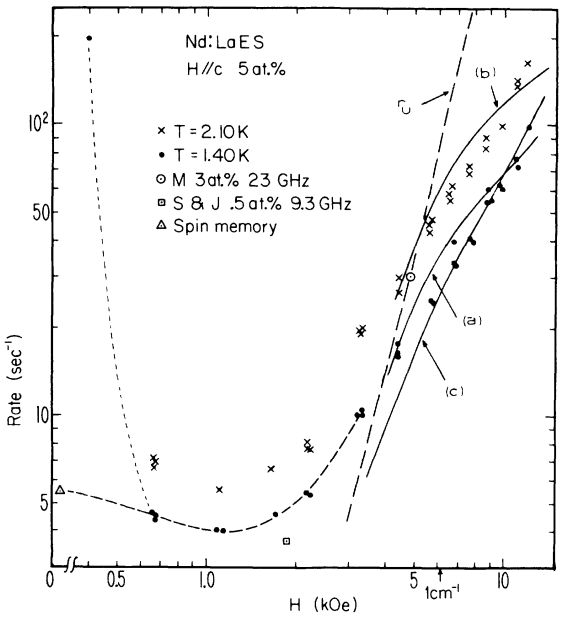

FIG. 11. Log_{10}-log_{10} plot of field dependence of the relaxation of 5-at.% Nd:LaES. Included for comparison are results of microwave saturation-recovery measurements taken at x- and k-band frequencies (Refs. 13 and 6) at a temperature of 1.4 °K. The departure of the slope of the field dependence in the high-field region from the predicted H^4 dependence is due to phonon bottleneck effects. A spin-memory measurement of the relaxation rate at zero current is shown. Curves drawn in the high-field region represent the use of Eq. (11) to fit the phonon-bottlenecked data.

the region in which local-field effects can influence the relaxation rate. Scott and Jeffries did, in fact, find a pronounced concentration dependence of the relaxation rate for Nd in their x-band measurements,[13] which is consistent with a local-field explanation. The slope of the high-field rate of Fig. 11 indicates that the phonon bottleneck is causing a departure from the H^4 dependence of spin-lattice theory, an interpretation consistent with the reduced rate measured in this study as compared to the microwave measurement made by the author[6] in which the Nd ion was found to be easily bottlenecked by increased microwave power. For this ion the fields achievable with the apparatus were sufficient to cause the splitting to become comparable to kT at 12 kOe, however the slope of the data exceeds that predicted by the $\delta^2 \coth^2(\delta/2kT)$ dependence of the strongly bottlenecked rate alone. Comparison with the microwave data shows that the rates obtained by the demagnetization method are not sufficiently depressed to fall into the strongly bottlenecked regime, hence Eq. (11) should be used. Since

the high-temperature approximation is not valid for this ion at these fields and temperatures, expressions (12) and (13) for r_b and r_u are appropriate. The solid curves drawn in the high-field region of Fig. 11 represents fits to Eq. (11) based on an unbottlenecked rate given by Eq. (13) with the coefficient $A' = 40.5\ \text{sec}^{-1}\,\text{cm}^5$. This unbottlenecked rate, determined by fitting a direct-process rate to the microwave data of Ref. 6, is shown by the dashed line in Fig. 11. Curves (a) and (b) are the results of the fitting process, using for r_b the Eq. (12) with a coefficient $D' = 13.2\ \text{sec}\,\text{cm}^2$. The resulting curves, based on the assumption of a field-independent phonon lifetime, are seen to exhibit a curvature which is not consistent with the experimental data. If, however, an inverse linear field dependence is assumed for the phonon lifetime, the improved fit shown by curve (c) is obtained. In this case, Eq. (12) has been modified to explicitly include the assumed field dependence of the phonon lifetime, giving the expression

$$r_b = D_1' \delta^3 \coth^2(\delta/2kT) \tag{17}$$

for the rate to be used in Eq. (11). For the curve shown, $D_1' = 8.0\ \text{sec}^{-1}\,\text{cm}^3$. At the highest fields the agreement is good, but at intermediate fields,

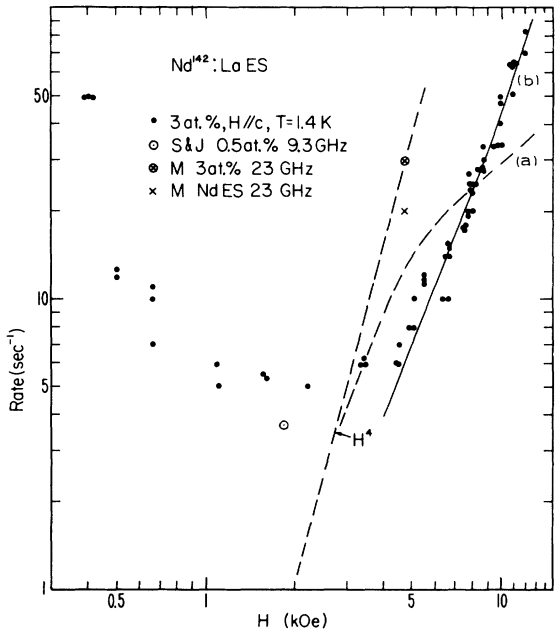

FIG. 12. Log_{10}-log_{10} plot of the field dependence of the relaxation rate of an even-isotope enriched sample of 3-at.% Nd:LaES. The results of microwave measurements (Refs. 13 and 6) are included for comparison, and the predicted H^4 dependence of an unbottlenecked rate is indicated. Curves drawn in the high-field region represent the use of Eq. (11) to fit the phonon-bottlenecked data.

around 4 KOe, the data depart from the above predictions. This is believed to be attributable to local-field corrections to the spin-lattice relaxation rate of the sort illustrated in Fig. 4. The field and temperature dependences of the phonon lifetime which are indicated by the fit are consistent, as for the case of the Sm sample, with the mechanism of diffusion to lattice defects.[29]

In the very-low-field region of Fig. 11 the data obtained by the demagnetization method show an abrupt increase in relaxation rate as the applied field is reduced to values of the order of the local fields of this ion (Table I). These rates are, however, not consistent with the rate at very low fields measured by the spin-memory method indicated by the triangular data point. As with the Sm ion, the spin-memory rate is believed to represent the true local-field-corrected spin-lattice rate (Fig. 4), and the anomalously rapid rates measured by the demagnetization method to be a result of a local-field disruption of the optical method of detection.

Figure 12 presents the measurement of the relaxation rate of an even-isotope enriched sample, 3-at.% ^{142}Nd:LaES. For this isotope the hyperfine field is absent, so the only local-field contribution is the dipolar field. A comparison of the low-field results for the two Nd samples (Figs. 11 and 12) shows only a subtle change in slope which may be indicative of the altered local field. This change is in qualitative agreement with the behavior which would be expected for the fields estimated in Table I.

The high-field data shown in Fig. 12 for the even-isotope enriched sample indicate that the relaxation of this sample is more strongly bottlenecked than the relaxation of the sample which had natural isotopic abundancies (Fig. 11). Attempts were made to fit the data in Fig. 12 to Eq. (11), again using for the unbottlenecked rate, r_u the expression given by Eq. (16) with the coefficient $A' = 40.5\ \text{sec}\,\text{cm}^5$; the approximate H^4 dependence of this unbottlenecked rate is drawn in the figure for comparison. Curve (a) in Fig. 12 shows an attempted fit which uses for r_b the expression given by Eq. (15) with field-independent coefficient $D' = 5.28\ \text{sec}\,\text{cm}^2$. The resulting curve indicates that the assumption of a field-independent phonon lifetime again does not provide an expression which fits the data. In addition the assumption of a linear field dependence for the phonon lifetime did not provide a good fit to the data. However, the assumption of a phonon lifetime having an inverse δ^2 dependence gave the good fit which is shown by the curve (b) in Fig. 12. This fit again represents the phonon-bottlenecked rate of Eq. (11), but uses for r_b the expression

$$r_b = D_2' \delta^4 \coth^2(\delta/2kT), \quad (18)$$

where Eq. (12) has been modified to include explicitly the assumed δ^2 dependence for the phonon lifetime. The fit shown by curve (b) uses for D_2' the value 2.93 $\text{sec}^{-1}\,\text{cm}^4$. The quality of agreement is good and could not be duplicated using other field dependences for the phonon lifetime.

Figure 13 presents the results of relaxation measurements on the Er ion in the ethylsulfate. Local-field effects dominate the measurements out to a field of 4 kOe, a field strength substantially larger than the averaged local field estimate of Table I. Thus the region of low fields for which an unexpected fast relaxation rate was measured does not correspond so closely with the estimated local fields of Table I for this ion as was encountered in the case of the Sm and Nd ions. In addition a pronounced cencentration dependence was observed for these measured rates. As for the other ions, these low-field rates are not believed to represent the true spin-lattice relaxation, but a feature unique to the optical method of detection. No spin-memory measurement was made on this sample. For the high-field measurements, the difference between the slopes hints that the concentrated sample is more strongly bottlenecked than the dilute sample, but high-fields would be necessary to clearly observe this effect. For this sample, r_b appears to be approximately 40 sec^{-1}.

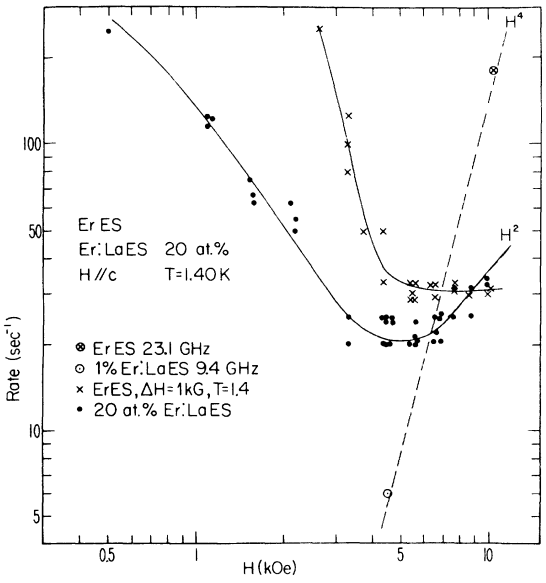

FIG. 13. Log_{10}-log_{10} plot of the field dependence of the relaxation of the Er ion in ErEs and in 20 at.% Er:LaES. Included is microwave data taken at x and k bands (Refs. 16 and 6) which conform to the expected H^4 dependence of theory. The departure of the data of this study from an H^4 dependence in the high-field region is due to the effect of the phonon bottleneck.

V. SUMMARY AND CONCLUSIONS

The combination of a pulsed magnetic field and optical detection has provided a useful method for the measurement of the field dependence of the relaxation of paramagnetic ions. The optical method permits the study of relaxation rates over a continuous range of fields, while the use of a superconducting magnet allows the achievement of high magnetic fields and fast pulsing. These features permitted the use of a spin-memory technique to measure spin-lattice relaxation rates at very low applied fields. The Sm:LaES sample exhibited a high-field relaxation rate in agreement with the theory for the field dependence of spin-lattice relaxation. In general, the crystals having the high concentrations often necessary when the optical method is used showed at high fields the effects of the phonon bottleneck. The field dependences in this case were interpreted by the application of the existing theory for the influence of the phonon bottleneck on the spin-lattice relaxation rate. Curve fitting of the data indicates a field-dependent phonon lifetime. Anomalous rates were measured with the optical method for fields of the order of local fields, but the true spin-lattice relaxation rates at zero current in the solenoid were measured by a spin-memory technique.

This study has shown the general capability of the approach used here for measuring the field dependence of the relaxation of paramagnetic ions, and has revealed the presence of effects such as the phonon bottleneck and spin-spin interactions, occuring in the high- and low-field regions, respectively, which cause departure of the measured rate from that predicted for the spin-lattice relaxation of an isolated ion. Modification of the apparatus to provide a magnet capable of rapid pulsing at higher fields or the selection of other samples might permit the observation of the phonon-bottlenecked rates in the strongly bottlenecked region. The spin-memory method, developed only in the late stages of this study, could be extended by circuitry modifications to allow the measurement of spin-lattice relaxation rates over the entire low-field region where the demagnetization method gives the anomalous rates found here. The resulting low-field spin-lattice rates could then be used to test the effective-field theories of spin lattice relaxation.[12,23,40,41]

The author thanks Dr. R. A. Satten for helpful discussions and for his encouraging interest in this work.

*Research supported in part by the N.S.F.

†Present address: Electro Optics Organization, GTE Sylvania Inc., Mountain View, Calif. 94042.

[1]J. M. Daniels and K. E. Riekhoff, Can. J. Phys. 38, 604 (1960).
[2]H. Kalbfleisch, Z. Phys. 181, 13 (1964).
[3]C. K. Asawa and R. A. Satten, Phys. Rev. 127, 1542 (1962).
[4]J. Wooldridge, Phys. Rev. 185, 602 (1969).
[5]E. S. Sabisky and C. H. Anderson, Phys. Rev. B 1, 2028 (1970).
[6]C. A. Moore and R. A. Satten, Phys. Rev. B 7, 1753 (1973).
[7]A. Abragam and W. G. Proctor, Phys. Rev. 109, 1441 (1958).
[8]U. Kump, Phys. Status Solidi 34, 691 (1969).
[9]D. J. Griffiths and H. Glattli, Can. J. Phys. 43, 2361 (1965).
[10]C. A. Moore, dissertation (UCLA, 1971) (unpublished).
[11]R. Orbach, Proc. R. Soc. Lond. A 264, 458 (1961).
[12]R. Orbach, Proc. R. Soc. Lond. A 264, 485 (1961).
[13]P. L. Scott and C. D. Jeffries, Phys. Rev. 127, 32 (1962).
[14]C. Y. Huang, Phys. Rev. 139, A241 (1962).
[15]R. C. Mikkelson and H. J. Stapleton, Phys. Rev. 140, A1968 (1965).
[16]G. H. Larson and C. D. Jeffries, Phys. Rev. 141, 461 (1966).
[17]G. H. Larson and C. D. Jeffries, Phys. Rev. 145, 311 (1966).
[18]M. B. Shulz and C. D. Jeffries, Phys. Rev. 149, 270 (1966).
[19]J. Van Den Broek and L. C. Van Der Marel, Physica (Utr.) 29, 948 (1963).
[20]A. Singh and R. C. Sapp, Phys. Rev. B 5 (1972).
[21]A. H. Cooke, C. B. P. Finn, B. W. Magnum, and R. L. Orbach, J. Phys. Soc. Jpn. 17, 462 (1962).
[22]D. A. Davids and P. E. Wagner, Phys. Rev. Lett. 12, 141 (1964).
[23]D. L. Huber, Phys. Rev. 131, 190 (1963).
[24]A. Sills, dissertation (UCLA), 1971 (unpublished).
[25]K. D. Bowers and J. Owen, Rep. Prog. Phys. 18, 304 (1955).
[26]H. Glattli, Can. J. Phys. 46, 103 (1968).
[27]H. Kalbfleisch, Phys. Status Solidi 34, 685 (1969).
[28]B. W. Faughnan and M. W. P. Strandberg, J. Phys. Chem. Solids 19, 155 (1961).
[29]A. M. Stoneham, Proc. Phys. Soc. Lond. 86, 1163 (1965).
[30]G. L. Pollack, Rev. Mod. Phys. 41, 48 (1969).
[31]R. E. Peterson and A. C. Anderson, J. Low Temp. Phys. 11, 639 (1973).
[32]L. J. Challis, J. Phys. C 7, 481 (1974).
[33]J. H. Van Vleck, Phys. Rev. 57, 426 (1940).
[34]M. Daniels, Proc. Phys. Soc. Lond. A 66, 673 (1953).
[35]R. Kronig and C. J. Bouwkamp, Physics 5, 521 (1938); 6, 290 (1939).
[36]N. Bloembergen, S. Shapiro, P. S. Pershan, and J. O. Artman, Phys. Rev. 114, 445 (1959); N. Bloembergen, Am. J. Phys. 41, 325 (1973).
[37]For a comprehensive review of the concept of spin temperature and its use in the interpretation of spin-spin interactions see M. Goldman, *Spin Temperature and Nuclear Magnetic Resonance in Solids* (Oxford U.P., London, 1970).
[38]R. W. Ditchburn, *Light* (Interscience, New York, 1963), Vol. 2, p. 569.
[39]J. Becquerel and W. J. DeHaas, Commun. Kamerlingh Onnes Lab. Univ. Leiden A 193 (1928).
[40]E. R. Bernstein and D. R. Franceschetti, Phys. Rev. B 6, 1654 (1972); 9, 3678 (1974).
[41]C. A. Hutchison, Jr., M. D. Kemple, and Y. T. Yen, Phys. Rev. Lett. 33, 937 (1974).